

1 **The gene *cortex* controls scale colour identity in *Heliconius***

2

3 **Luca Livraghi^{1,2}, Joseph J. Hanly^{1,2,3}, Ling Sheng Loh², Anna Ren², Ian A. Warren¹, Carolina**
4 **Concha², Charlotte Wright¹, Jonah M. Walker¹, Jessica Foley², Henry Arenas-Castro², Lucas**
5 **Rene Brenes², Arnaud Martin³, W. Owen McMillan² and Chris D. Jiggins^{1,2}**

6

7 **Author affiliations:**

- 8 1. Department of Zoology, University of Cambridge, Downing St., Cambridge, CB2 3EJ, UK
9 2. Smithsonian Tropical Research Institute, Gamboa, Panama
10 3. The George Washington University Department of Biological Sciences, Science and
11 Engineering Hall 6000, 800 22nd St NW Washington, DC 20052, USA

12

13 **Corresponding author:** Luca Livraghi, University of Cambridge, Cambridge, UK. Dept. of Zoology.
14 ll566@cam.ac.uk.

15 **Funding:**

16 This work was funded by a grant from the BBSRC to CJ and supported LL (BB/R007500/1); the
17 National Science Foundation awards IOS-1656553 and IOS-1755329 to AM; a Wellcome Trust PhD
18 studentship awarded to JJH, a Smithsonian Institution grant to WOM and a Balfour-Browne Trust
19 studentship to J.M.W.

20 **Keywords:**

21 Evolution, wing patterning, *cortex*, *Heliconius*, cell fate, CRISPR, Lepidoptera.

22 **Abstract**

23 The wing patterns of butterflies are an excellent system with which to study phenotypic evolution. The
24 incredibly diverse patterns are generated from an array of pigmented scales on a largely two-
25 dimensional surface, resulting in a visibly tractable system for studying the evolution of pigmentation.
26 In *Heliconius* butterflies, much of this diversity is controlled by a few genes of large effect that regulate
27 pattern switches between races and species across a large mimetic radiation. One of these genes – *cortex*
28 - has been repeatedly mapped in association with colour pattern evolution in both *Heliconius* and other
29 Lepidoptera, but we lack functional data supporting its role in modulating wing patterns. Here we
30 carried out CRISPR knock-outs in multiple *Heliconius* species and show that *cortex* is a major
31 determinant of scale cell identity. Mutant wing clones lacking *cortex* showed shifts in colour identity,
32 with melanic and red scales acquiring a yellow or white state. These homeotic transformations include
33 changes in both pigmentation and scale ultrastructure, suggesting that *cortex* acts during early stages of
34 scale cell fate specification rather than during the deployment of effector genes. In addition, mutant
35 clones were observed across the entire wing surface, contrasting with other known *Heliconius* mimicry
36 loci that act in specific patterns. Cortex is known as a cell-cycle regulator that modulates mitotic entry
37 in *Drosophila*, and we found the Cortex protein to accumulate in the nuclei of the polyploid scale
38 building cells of the butterfly wing epithelium, speculatively suggesting a connection between scale cell
39 endocycling and colour identity. In summary, and while its molecular mode of action remains
40 mysterious, we conclude that *cortex* played key roles in the diversification of lepidopteran wing patterns
41 in part due to its switch-like effects in scale identity across the entire wing surface.

42

43 Introduction

44 Evolutionary hotspots have become a recurrent theme in evolutionary biology, whereby variation
45 surrounding homologous loci at both micro- and macro-evolutionary scales have driven parallel cases
46 of phenotypic change. Notably, a remarkable 138 genes have been linked to phenotypic variation in 2
47 or more species (GepheBase; Courtier-Orgogozo et al., 2020). In some cases, parallel adaptation has
48 occurred through the alteration of downstream effector genes, such as pigmentation enzymes with
49 functions clearly related to the trait under selection (e.g. *tan*, *ebony*). In other cases, upstream patterning
50 factors are important, and these are typically either transcription factors (e.g. *optix*, *pitx1*, *Sox10*) or
51 components of signalling pathways such as ligands or receptors (e.g. *WntA*, MC1R). These classes of
52 genes influence cell fate decisions during development by modulating downstream gene regulatory
53 networks (Kronforst and Papa, 2015; Martin and Courtier-Orgogozo, 2017; Prud'homme et al., 2007),
54 and are commonly characterised by highly conserved functions, with rapid evolutionary change
55 occurring through regulatory fine-tuning of expression patterns. One gene that has been repeatedly
56 implicated in morphological evolution but is conspicuous in its failure to conform to this paradigm is
57 *cortex*, a gene implicated in the regulation of adaptive changes in the wing patterning of butterflies and
58 moths.

59 *Cortex* is one of four major effect genes that act as switch loci controlling both scale structure and colour
60 patterns in *Heliconius* butterflies, and has been repeatedly targeted by natural selection to drive
61 differences in pigmentation (Nadeau, 2016; Van Belleghem et al., 2017). Three of the four major effect
62 genes correspond to the prevailing paradigm of highly conserved patterning genes; the signalling ligand
63 *WntA* (Concha et al., 2019; Mazo-Vargas et al., 2017) and two transcription factors *optix* (Lewis et al.,
64 2019; Zhang et al., 2017) and *aristaless1* (Westerman et al., 2018). The fourth is *cortex*, an insect-
65 specific gene showing closest homology to the *cdc20/fizzy* family of cell cycle regulators (Chu et al.,
66 2001; Nadeau et al., 2016; Pesin and Orr-Weaver, 2007). The lepidopteran orthologue of *cortex* displays
67 rapid sequence evolution, and has acquired novel expression domains that correlate with melanic wing
68 patterns (Nadeau et al., 2016; Saenko et al., 2019). It therefore seems likely that the role of *cortex* in
69 regulating wing patterns has involved a major shift in function, which sits in contrast to the classic
70 model of regulatory co-option of deeply conserved patterning genes, that can be readily applied to other
71 major *Heliconius* patterning loci.

72 The genetic locus containing *cortex* was originally identified in the genus *Heliconius* as controlling
73 differences in yellow and white wing patterns in *H. melopmene* and *H. erato* (Figure 1a) and the
74 polymorphism in yellow, white, black and orange elements in *H. numata*, using a combination of
75 association mapping and gene expression data (Joron et al., 2006; Nadeau et al., 2016). The same locus
76 has also been repeatedly implicated in controlling colour pattern variation among divergent
77 Lepidoptera, including the peppered moth *Biston betularia* and other geometrids, the silkmoth *Bombyx*

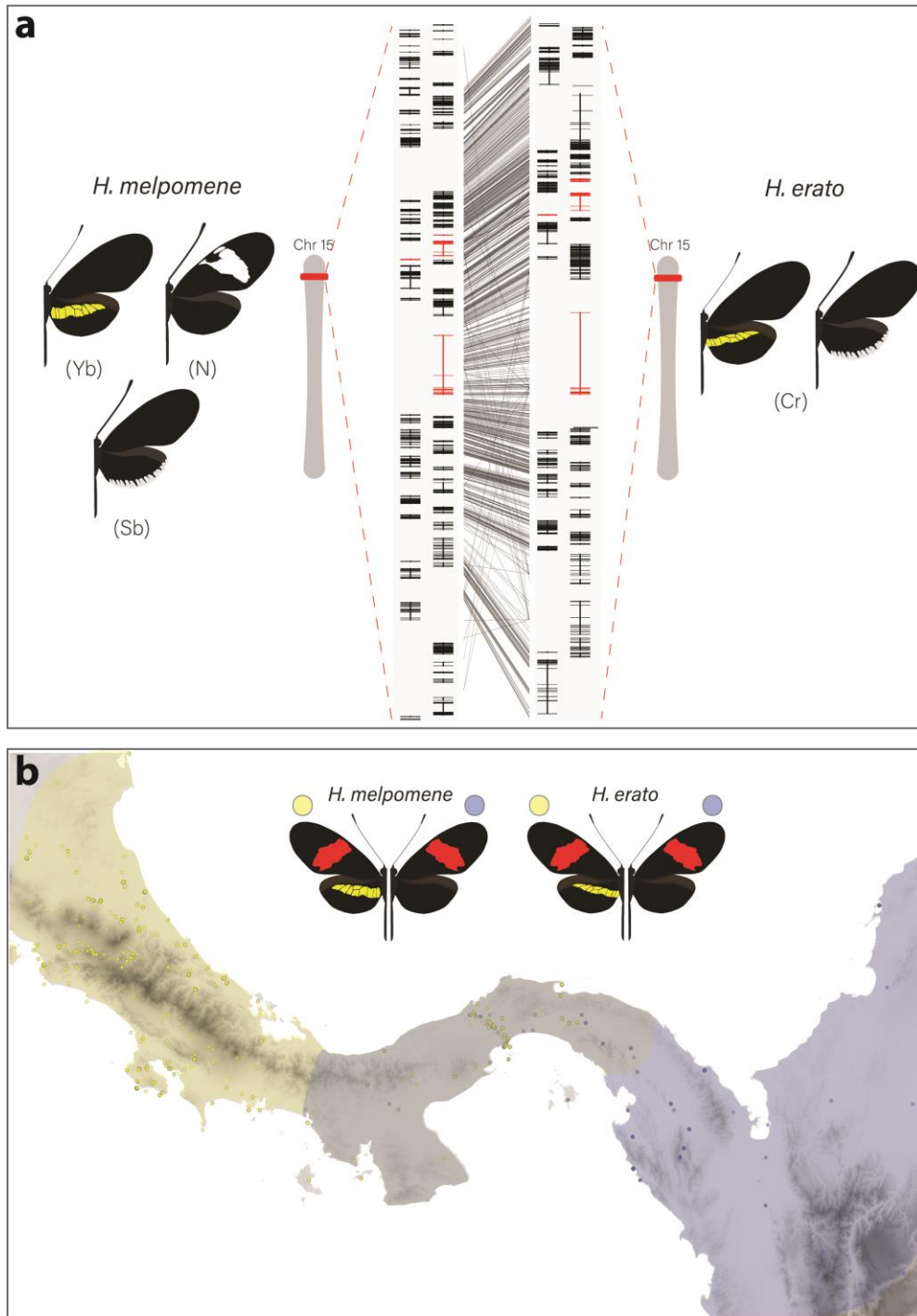
78 *mori* and other butterflies such as *Bicyclus anynana* and *Papilio clytia* (Beldade et al., 2009; Ito et al.,
79 2016; VanKuren et al., 2019; Van't Hof et al., 2019; Van't Hof et al., 2016). This locus therefore
80 contains one or more genes that have repeatedly been targeted throughout the evolutionary history of
81 the Lepidoptera to generate phenotypic diversity.

82 While *cortex* remains the most likely candidate driving yellow and white scale evolution in *Heliconius*,
83 other genes at the locus may also be playing a role in establishing scale colour identity. Most notably,
84 the genes *domeless* (*dome*), a JAK-STAT pathway receptor and *washout* (*wash*), a cytoskeleton
85 regulator, which also show associations with colour pattern phenotypes in *H. melpomene* and *H. numata*
86 (Nadeau et al., 2016; Saenko et al., 2019). These genes neighbour a non-coding region linked to the
87 Bigeye mutation in *B. anynana*, have been implicated in shaping eyespot patterns in CRISPR
88 mutagenesis experiments, and are within an interval of around 100kb which also includes *cortex*
89 (Beldade et al., 2009; Lopes da Silva, 2015). It is thus possible that multiple linked genes are
90 contributing to the evolution of wing patterning across Lepidoptera (Joron et al., 2006; Saenko et al.,
91 2019).

92 While fantastically diverse, most of the pattern variation in *Heliconius* is created by the differences in
93 the distribution of only three major scale cell types; Type I (yellow/white), Type II (black), and Type
94 III (red/orange/brown) (Aymone et al., 2013; Gilbert et al., 1987). Each type has a characteristic
95 nanostructure and a fixed complement of pigments. Type I yellow scales contain the ommochrome
96 precursor 3-hydroxykynurenine (3-OHK) (Finkbeiner et al., 2017; Koch, 1993; Reed et al., 2008),
97 whereas Type I white scales lack pigment, and the colour is the result of the scale cell morphology (i.e.
98 structural) (Gilbert et al., 1987). In contrast, Type II scale cells are pigmented with melanin and Type
99 III scale cells contain the red ommochrome pigments xanthommatin and dihydroxanthommatin.

100 Here we focus on the role of *cortex* in *Heliconius* butterflies, an adaptive radiation with over 400
101 different wing forms in 48 described species (Jiggins, 2017; Lamas, 2004) and where diversity in wing
102 patterns can be directly linked to the selective forces of predation and sexual selection (Brown, 1981;
103 Turner, 1981). Specifically, we combine expression profiling using *RNA-seq*, *in situ* hybridization and
104 antibody staining experiments, as well as CRISPR/Cas9 gene knock-outs to determine the role that this
105 locus plays in pattern variation of two co-mimetic races of *H. melpomene* and *H. erato* (Figure 1b).

106 Despite the fact that *cortex* does not follow the prevailing paradigm of patterning loci, we demonstrate
107 for the first time that the gene plays a fundamental role in pattern variation by modulating a switch from
108 Type I scale cells to Type II and Type III scale cells. Moreover, we show that the phenotypic effects of
109 *cortex* extend across the fore- and hindwing surface. Our findings, coupled with recent functional
110 experiments on other *Heliconius* patterning loci, are beginning to illuminate how major patterning genes
111 interact during development to determine scale cell fate and drive phenotypic variation across a
112 remarkable adaptive radiation.



113

Figure 1 – Ranges of *Heliconius* butterflies differing at Yb phenotypes in Central America and associated loci

(a) Homologous loci in both species are associated with variation in yellow and white patterns between races. In *H. melpomene* three tightly linked genetic elements located at chromosome 15 control variation for hindwing yellow bar, forewing band and white margin elements (Yb, N and Sb respectively) while in *H. erato* variation has been mapped to one element (Cr). Genes previously associated with wing patterning differences in Lepidoptera are highlighted in red within a specific region of chromosome 15 (from bottom up; *cortex*, *domeless-truncated*, *domeless* and *washout*) and alignment between the two co-mimetic species at the locus is shown (grey lines, 95% alignment identity). (b) Focal co-mimetic races of *Heliconius erato* and *Heliconius melpomene* used in this study, differing for the presence of a hindwing yellow bar, and their ranges across Central America are shown (ranges based on Rosser et al., 2012). Yellow: yellow banded races, blue: black hindwing races, grey: range overlap.

114 Results

115 **RNA-seq and reannotation of key intervals reveals the presence of duplications and bi-cistronic** 116 **transcription of candidate genes**

117 In order to identify genes associated with differences in yellow pattern elements, we performed
118 differential gene expression (DGE) analysis using developing wings sampled from colour pattern races
119 in *H. erato* and *H. melpomene* differing only in the presence or absence of the hindwing yellow bar
120 (Figure 1b and Figure 2a). In total, we sequenced 18 samples representing three developmental stages
121 (larval, 36h +/-1.5h (Day 1 pupae) and 60h +/- 1.5h (Day 2 pupae)) from two races in each of the two
122 species, with hindwings divided into two parts for the pupal stages (Figure 2a). We focused our attention
123 on genes centred on a 47-gene interval on chromosome 15 previously identified as the minimal
124 associated region with yellow band phenotypes by recombination mapping (Nadeau et al., 2016, supp
125 table 1; Joron et al., 2006; Moest et al., 2020; Van Belleghem et al., 2017). Both our initial expression
126 analysis and recent analysis of selective sweeps at this locus (Moest et al., 2020) indicate that three
127 genes showed differential expression and are likely targets of selection: *cortex*, *dome* and *wash* (Figure
128 2c). This led us to further explore the annotation of these genes prior to further analysis.

129 In *Heliconius*, *dome* appears to have duplicated in the ancestor of *H. erato* and *H. melpomene*, resulting
130 in a full-length copy (referred to here as *domeless*) and a further copy exhibiting truncations at the C-
131 terminus (*domeless-truncated*) (Supplementary File 1 – Figure S1). Independent tandem duplications
132 of *dome* have occurred in several other Lepidoptera. Protein alignments indicate that in both *H. erato*
133 and *H. melpomene*, *dome-trunc* maintains only the N-terminal half of the gene, suggesting *dome-trunc*
134 is undergoing pseudogenisation.

135 When examining the *RNA-seq* reads mapping to the *dome* and *wash* genes, we observed several
136 individual reads splicing over the 5' UTR of *wash* and into the coding region of *dome*. It was not
137 possible to unambiguously assign reads that map to this overlapping portion of the annotation to either
138 gene, suggesting the possibility that *dome/wash* are transcribed as a single, bi-cistronic transcript. To
139 look for further evidence of co-transcription, we searched the Transcription Shotgun Assembly (TSA)
140 sequence archive on NCBI for assembled transcripts containing the open reading frames (ORFs) of both
141 genes in other Lepidoptera (Supplementary File 2 – Figure S2). We found several instances where ORFs
142 encoding for both *dome* and *wash* can be found in a single transcript, suggesting bi-cistronic
143 transcription is a conserved feature across butterflies. Furthermore, an examination of published *ATAC-*
144 *seq* peaks (Lewis et al., 2019), shows the presence of a single promoter at the start of *dome* for *H. erato*
145 *lativitta*, suggesting both genes share a single transcription start site (Supplementary File 2 – Figure
146 S2). Given this result, we repeated the DGE analysis with *dome/wash* as a single annotation.

147 **The genes *cortex* and *domeless/washout* are differentially expressed between colour pattern races,**
148 **and between wing sections differing in the presence of the hindwing yellow bar**

149 *RNA-seq* data show *cortex* transcripts were most abundant in 5th instar larvae, almost depleted in Day 1
150 pupae, but were again detected at relatively high levels in Day 2 pupae in *H. melpomene*, suggesting
151 dynamic expression in this species (Figure 2b). In *H. erato*, *cortex* transcripts are found in high
152 abundance in 5th instar larvae but are almost depleted in Day 1 and Day 2 pupae. Both *dome* paralogs
153 remain relatively constant in terms of expression across all stages in *H. melpomene* whereas *dome-trunc*
154 expression increases in pupal stages in *H. erato*. *Dome/wash* transcripts are detected in relatively low
155 and constant amounts in both species.

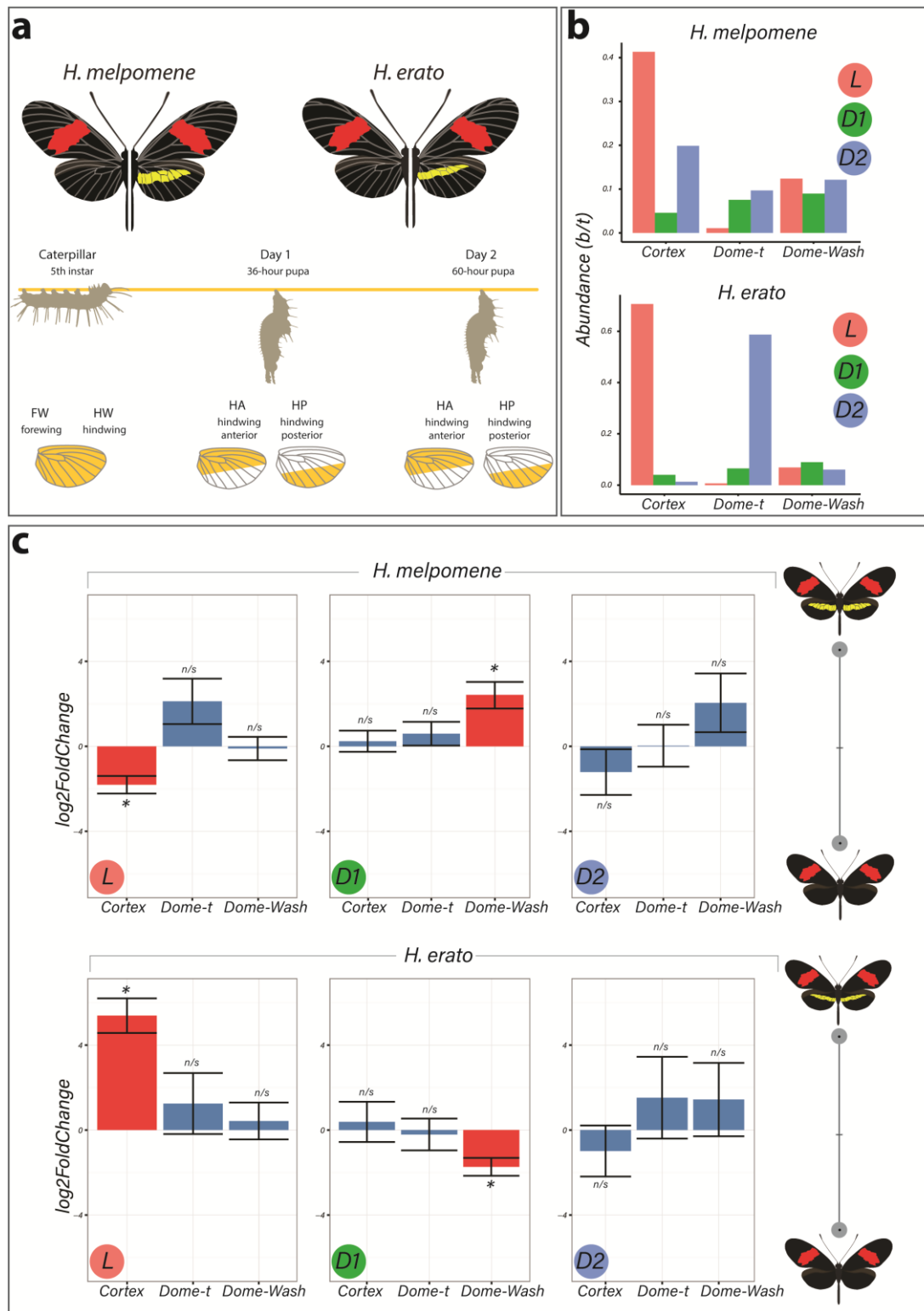
156 The two species were analysed separately, with both showing only *cortex* and *dome/wash* as
157 significantly differentially expressed between morphs among the 47 genes in the candidate region, with
158 *cortex* differential expression occurring earlier in development. In fifth instar larvae, *cortex* is
159 differentially expressed in both species between the two colour pattern races, with *cortex* showing the
160 highest adjusted *p*-value for any gene in the genome at this stage in *H. erato* (Figure 2c). Interestingly,
161 *cortex* transcripts were differentially expressed in opposite directions in the two species, with higher
162 expression in the melanic hindwing race in *H. melpomene*, and in the yellow banded race in *H. erato*.
163 This pattern is reversed for *dome/wash* in Day 1 pupae, where a statistically higher proportion of
164 transcripts are detected in *H. melpomene rosina* (yellow), and in *H. erato hydara* (melanic). No
165 differential expression of these genes was found at Day 2 pupae. In order to confirm this inverted pattern
166 was not due to a sampling error, we performed a diagnostic SNP analysis by correlating coding SNPs
167 found within protein coding genes at the *cortex* locus from whole genome sequence data to the
168 corresponding *RNA-seq* datasets (Supplementary File 3 – Tables S3.1 and S3.2).

169 When comparing across hindwing sections differing for the yellow bar phenotype, 22 genes out of the
170 associated 47-gene interval were differentially expressed at Day 1 between relevant wing sections in *H.*
171 *melpomene*, including *cortex* and *dome/wash* (Supplementary File 4 – Figures S4.1 and S4.2). In
172 contrast in *H. erato* Day 1 pupae, only *dome/wash* was differentially expressed. At Day 2 pupae, there
173 were no differentially expressed genes in either species between relevant wing sections at this locus.

174 Given the strong support for the involvement of *cortex* in driving wing patterning differences, we re-
175 analysed its phylogenetic relationship to other *cdc20* family genes with more extensive sampling than
176 previous analyses (Nadeau et al., 2016). Our analysis finds strong monophyletic support for *cortex* as
177 an insect-specific member of the *cdc20* family, with no clear *cortex* homologs found outside of the
178 Neoptera (Supplementary File 5 – Figure S5.1). Branch lengths indicate *cortex* is evolving rapidly
179 within the lineage, despite displaying conserved APC/C binding motifs, including the C-Box and IR
180 tail (Supplementary File 5 – Figure S5.2) (Chu et al., 2001; Pesin and Orr-Weaver, 2007).

181 In summary, *cortex* is the most consistently differentially expressed gene and showed differential
 182 expression earlier in development as compared to the other candidate *dome/wash*. We therefore focus
 183 subsequent experiments on *cortex*, although at this stage we cannot rule out an additional role for
 184 *dome/wash* in pattern specification.

185



186

Figure 2 – Differential expression of genes at Chromosome 15 implicate *cortex* as most likely candidate driving yellow bar differences

(a) Hindwing tissue from co-mimetic races of *H. melpomene* and *H. erato* were collected at three developmental stages (5th instar caterpillar, Day 1 Pupae (36hAPF) and Day 2 Pupae (60hAPF)). For pupal tissue, hindwing tissue was dissected using the wing vein landmarks shown, corresponding to the future adult position of the hindwing yellow bar (dissection scheme based on Hanly et al., 2019). (b) Relative abundance of transcripts corresponding to the genes *cortex*, *domeless-truncated*, *domeless/washout* throughout developmental stages. *Cortex* expression decreases from larval to pupal stages *domeless-truncated* expression increases, whereas *domeless/washout* stay relatively constant at all three stages. (c) Log₂FoldChange for the genes *cortex*, *domeless-truncated*, *domeless/washout* across developmental stages. Comparisons are for whole wing discs (Larvae, L) and for contrast C for pupae (D1 and D2; see Supplementary File 4: Figure S4.3 for depiction of contrasts analysed).

187

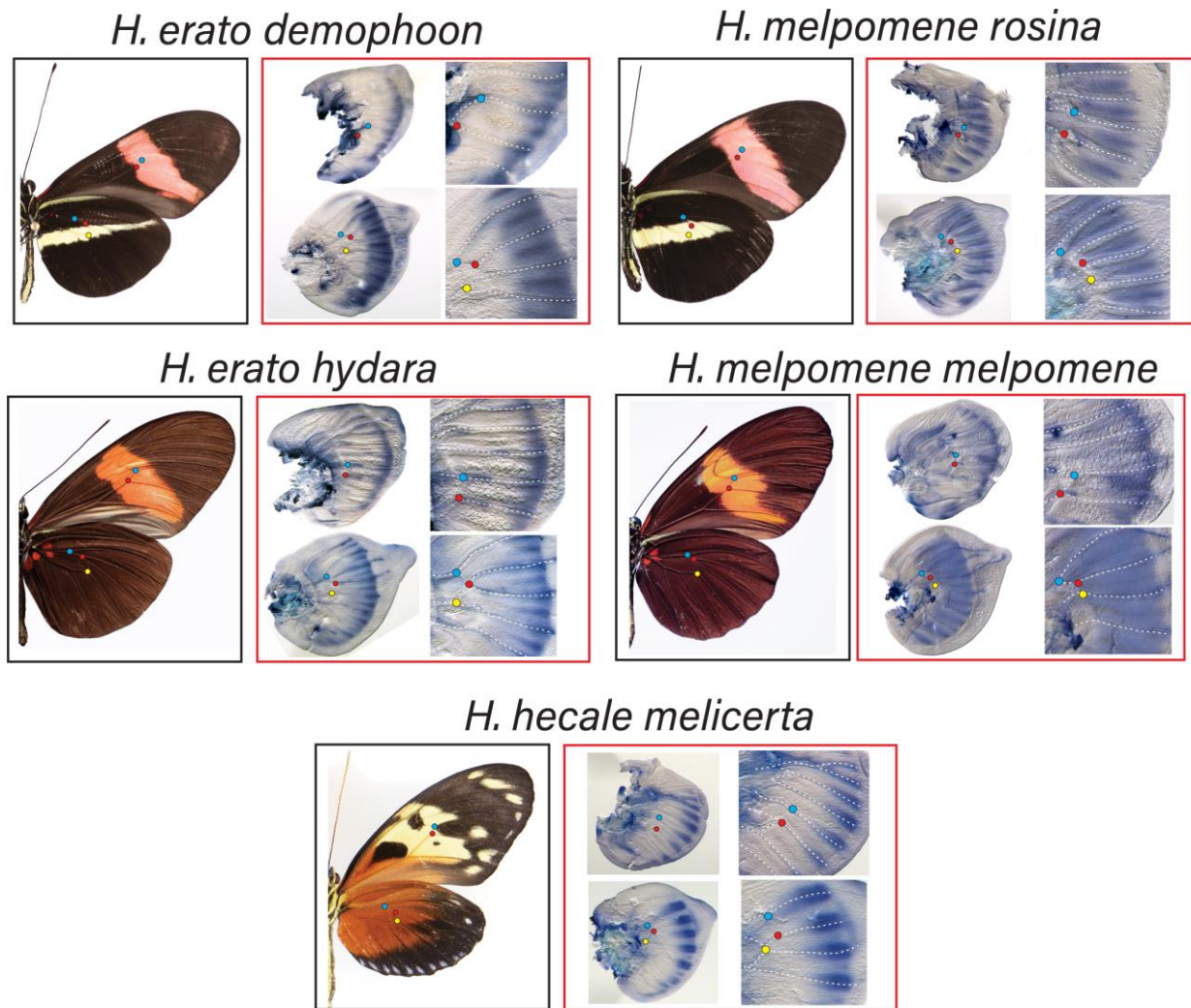
188 ***Cortex* transcripts localise distally in 5th instar larvae**

189 Two studies have reported that *cortex* mRNA expression correlates with melanic patch in two species
190 of *Heliconius* (Nadeau et al., 2016 and Saenko et al., 2019). To further assess this relationship between
191 *cortex* expression and adult wing patterns, we performed *in situ* hybridisation on developing wing discs
192 of 5th instar larvae, where we observed largest *cortex* transcript abundance, in both the yellow-barred
193 and plain hindwing morphs of *H. erato* and *H. melpomene*. *Cortex* transcripts at this stage localised
194 distally in forewings and hindwings of both species (Figure 3). In *H. erato demophoon*, expression was
195 strongest at the intervein midline, but extends across vein compartments covering the distal portion of
196 both forewing and hindwing. By contrast, in *H. erato hy dara*, *cortex* transcripts are more strongly
197 localised to the intervein midline forming a distally localised intervein expression domain.

198 Expression in *H. melpomene rosina* is similar to *H. erato demophoon* at comparable developmental
199 stages, again with stronger expression localised to the intervein midline but extending further
200 proximally than in *H. erato demophoon*. In *H. melpomene melpomene*, hindwing *cortex* expression
201 extends across most of the hindwing, and does not appear to be restricted to the intervein midline.

202 Given that *cortex* has been implicated in modulating wing patterns in many divergent lepidoptera, we
203 examined localisation in a *Heliconius* species displaying distinct patterns: *H. hecale melicerta* (Figure
204 3). Interestingly, in this species transcripts appear strongest in regions straddling the wing disc veins,
205 with weak intervein expression observed only in the hindwings. Previous data has shown variation in
206 yellow spots (Hspot) is also controlled by a locus located a chromosome 15 (Huber et al., 2015).
207 Expression in *H. hecale melicerta* forewings corresponds to melanic regions located in between yellow
208 spots at the wing margins, indicating *cortex* may be modulating Hspot variation in *H. hecale*.

209 Overall, our results suggest a less clear correlation to melanic elements than reported expression
210 patterns (Nadeau et al., 2016; Saenko et al., 2019) where *cortex* expression in 5th instar caterpillars is
211 mostly restricted to the distal regions of developing wings, but appears likely to be dynamic across 5th
212 instar development.



213

Figure 3 – Expression of *cortex* transcripts in *H. melpomene*, *H. erato* and *H. hecale* 5th instar wing discs

Cortex expression in 5th instar wing discs is restricted to the distal end of both forewings and hindwings in all species and morphs analysed. In *H. erato*, expression is strongest at the intervein midline but extends across vein compartments in *H. erato demophoon*, whereas it is more strongly localised to the intervein midline in *H. erato hydara*. In *H. melpomene rosina*, *cortex* localises in a similar manner to *H. erato demophoon*, with stronger expression again observed at the intervein midline, whereas expression in *H. melpomene melpomene* extends more proximally. Coloured dots represent homologous vein landmarks across the wings.

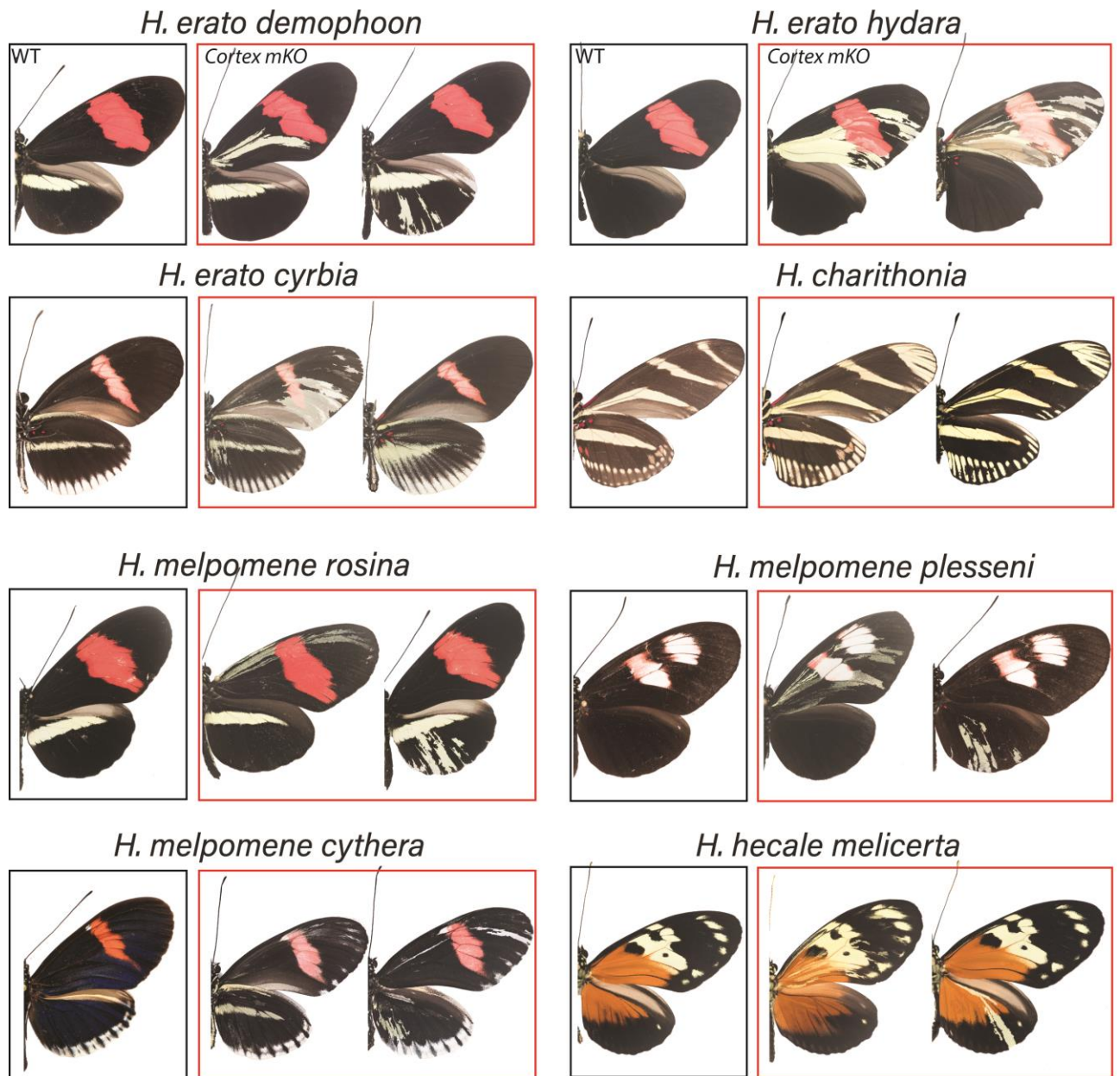
214 ***Cortex* establishes Type II and III scale identity in *Heliconius* butterflies**

215 To assay the function of *cortex* during wing development, we used CRISPR/Cas9 to generate G₀
216 somatic mosaic mutants (crispants) (Mazo-Vargas et al., 2017; Zhang et al., 2017). We targeted
217 multiple exons using a combination of different guides and genotyped the resulting mutants through
218 PCR amplification, cloning and Sanger sequencing (Supplementary File 6 – Figure S6). Overall KO
219 efficiency was low when compared to similar studies in *Heliconius* (Concha et al., 2019; Mazo-Vargas
220 et al., 2017), with observed wing phenotype to hatched eggs ratios ranging from 0.3% to 4.8%. Lethality

221 was also high, with hatched to adult ratios ranging from 8.1% to 29.8% (Supplementary File 7 – Table
222 S7.1).

223 Targeting of the *cortex* gene in *H. erato* produced patches of ectopic yellow and white scales spanning
224 regions across both forewings and hindwings (Figure 4 and Supplementary File 8 – Figures S8.1-S8.7).
225 Both colour pattern races were affected in a similar manner in *H. erato*. Mutant clones were not
226 restricted to any specific wing region, affecting scales in both proximal and distal portions of wings.
227 The same effect on scale pigmentation was also observed in the co-mimetic morphs in *H. melpomene*,
228 with mutant clones affecting both distal and proximal regions in forewings and hindwings. In *H. erato*
229 *hydara*, we recovered a mutant individual where clones spanned the dorsal forewing band. Clones
230 affecting this region caused what appears to be an asymmetric deposition of pigment across the scales,
231 as well as transformation to white, unpigmented scales (Figure 5 and Supplementary File 9 – Figure
232 S9).

233 As this locus has been associated with differences in white hindwing margin phenotypes (Jiggins and
234 McMillan, 1997) (Figure 1b), we also targeted *cortex* in mimetic races showing this phenotype, *H. erato*
235 *cyrbia* and *H. melpomene cythera*. Mutant scales in these colour pattern races were also localised across
236 both wing surfaces, with both white and yellow ectopic scales. In these races, a positional effect was
237 observed, where ectopic scales in the forewing and anterior compartment of the hindwing shifted to
238 yellow, and posterior hindwing scales became white (Figure 4 and Supplementary File 9 – Figure S9).
239 This positional effect likely reflects differential uptake of the yellow pigment 3-OHK across the wing
240 surface (Reed et al., 2008). For one individual of *H. erato cyrbia*, clones also extended across the red
241 band where a shift to white scales was observed, as in *H. erato hydara*.



242

Figure 4 – *Cortex* loss of function transforms scale identity across the entire wing surface

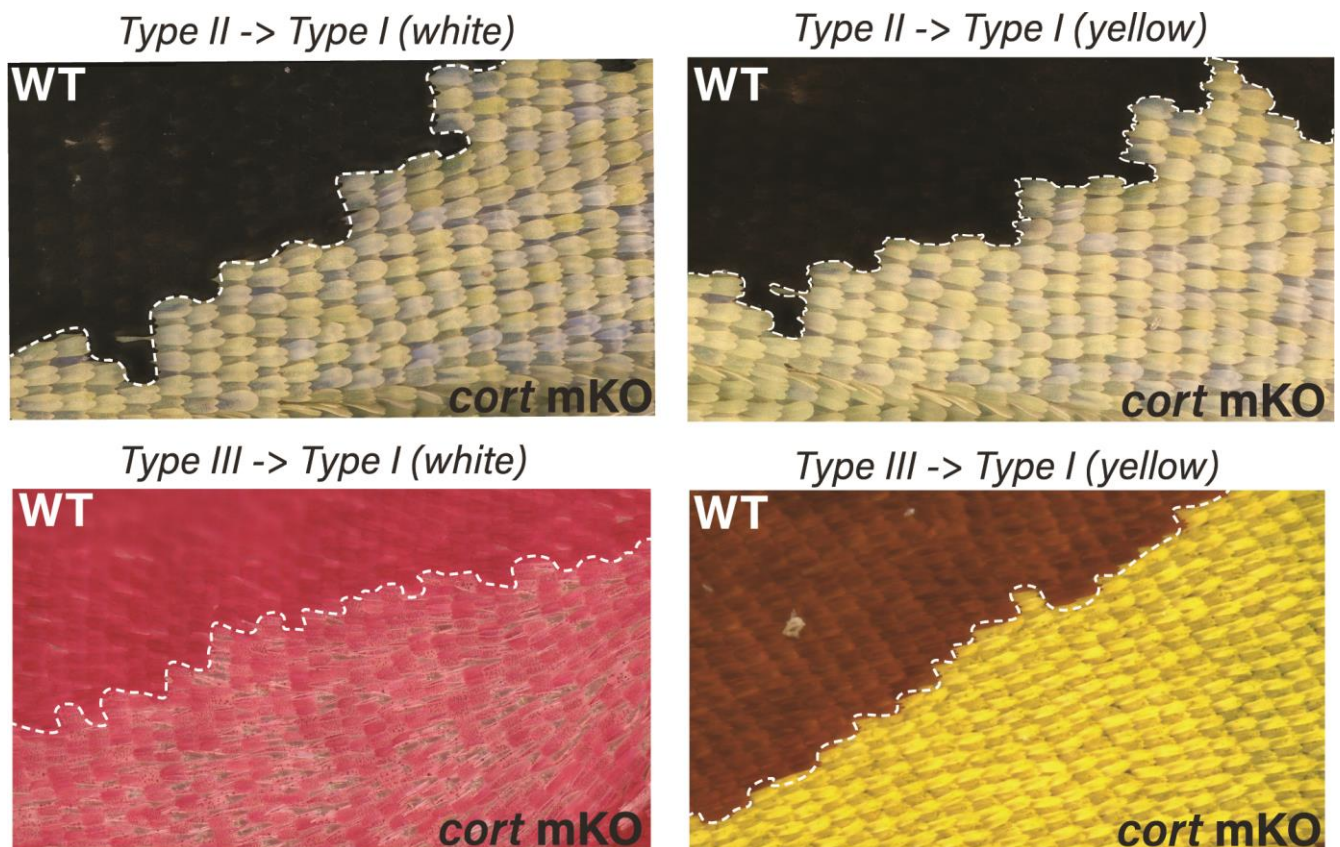
Phenotypes of *cortex* mKO across *Heliconius* species and morphs reveals a loss of melanic (Type II) and red (Type III) scales, and transformation to Type I (yellow or white) scales. Affected regions are not spatially restricted, and span both distal and proximal portions of forewings and hindwings. A positional effect is observed in some races, where ectopic Type I scales are either white or yellow depending on their position along the wing (e.g. *H. erato cyrbia*). Ectopic Type I scales can be induced from both melanic and red scales, switching to either white or yellow depending on wing position and race. Boundaries between Wild-type (WT) to mutant scales are highlighted (dotted white line).

243 To further test the conservation of *cortex* function across the *Heliconius* radiation, we knocked out
244 *cortex* in *H. charithonia* and *H. hecale melicerta*, outgroups to *H. erato* and *H. melpomene* respectively.
245 Again, ectopic yellow and white scales appeared throughout the wing surface in both species,
246 suggesting conserved function with respect to scale development among *Heliconius* butterflies. In *H.*

247 *hecale melicerta*, we also recovered a mutant where we saw transformation from orange ommochrome
248 scales to yellow.

249 In summary, *cortex* crispants appear to not be restricted to any specific wing pattern elements, and
250 instead affect regions across the surface of both forewings and hindwings. Mutant scales are always
251 Type I scales, with differing pigmentation (3-OHK, yellow) or structural colouration (white) depending
252 on race and wing position (Figure 5). The high rate of mosaicism combined with high mortality rates
253 suggests *cortex* is likely developmentally lethal. Furthermore, the sharp boundaries observed between
254 wild-type and mutant scales suggest *cortex* functions in a cell-autonomous manner, with little or no
255 communication between neighbouring cells (Figure 5 and Supplementary File 9 - Figure S9).

256



257

258

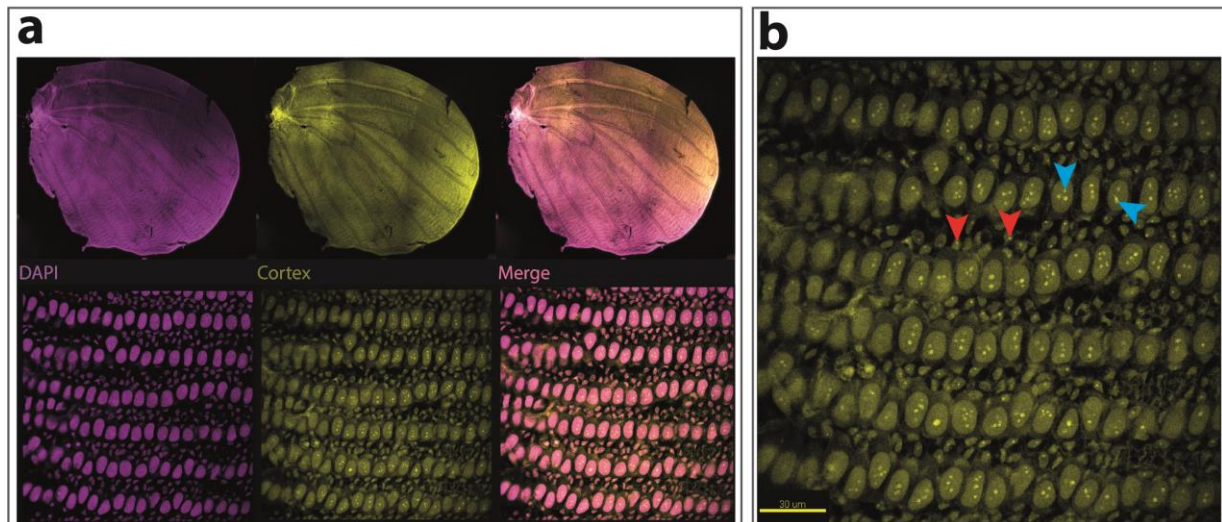
Figure 5 – CRISPR KOs induce Type I scale identity

Ectopic Type I scales can be induced from both melanic and red scales, switching to either white or yellow depending on wing position and race. Boundaries between Wild-type (WT) to mutant scales are highlighted (dotted white line).

259 **Nuclear localization of Cortex extends across the wing surface in pupal wings**

260 The *cortex* mRNA expression patterns in larval imaginal disks suggest a dynamic progression in the
261 distal regions, and in a few cases (Figure 3; Nadeau et al., 2016; Saenko et al., 2019) a correlation with
262 melanic patterns whose polymorphisms associate with genetic variation at the Cortex locus itself. We
263 thus long hypothesized that like for the *WntA* mimicry gene (Martin et al., 2012, Mazo-Vargas 2017 et
264 al., Concha et al., 2020), the larval expression domains of *cortex* would delimit the wing territories
265 where it is playing an active role in colour patterning. However, our CRISPR based loss-of-function
266 experiments challenge that hypothesis because in all the morphs that we assayed, we found mutant
267 scales across the wing surface (Figure 6 and supplementary File 9 – Figure S9).

268 This led us to re-examine our model and consider that post-larval stages of Cortex expression could
269 reconcile the observation of scale phenotypes across the entire wing, rather than in limited areas of the
270 wing patterns. To test this hypothesis, we developed a Cortex polyclonal antibody, and found nuclear
271 expression across the epithelium of *H. erato demophoon* pupal hindwings without restriction to specific
272 pattern element (Figure 6). This nuclear localization overlapped with DNA, also included a strong signal
273 in the large nucleoli of both the polyploid scale building cells, and their adjacent, non-polyploid
274 epithelial cells (Greenstein, 1972). Following previous reports suggesting a correlation between
275 pigmentation state and ploidy level (Cho and Nijhout, 2013; Henke and Pohley, 1952; Iwata and Otaki,
276 2016), we tested if nuclear volume or nucleoli number would associate with the yellow band, but failed
277 to find a consistent pattern in the distribution of Cortex protein (Figure 6 and Supplementary File 10 -
278 Figure S10). However, currently we cannot rule an association of Cortex protein with colour pattern
279 elements at other developmental stages, and given the apparent dynamic nature of *cortex* expression, a
280 more precise developmental time series will be required to make more conclusive statements.



281

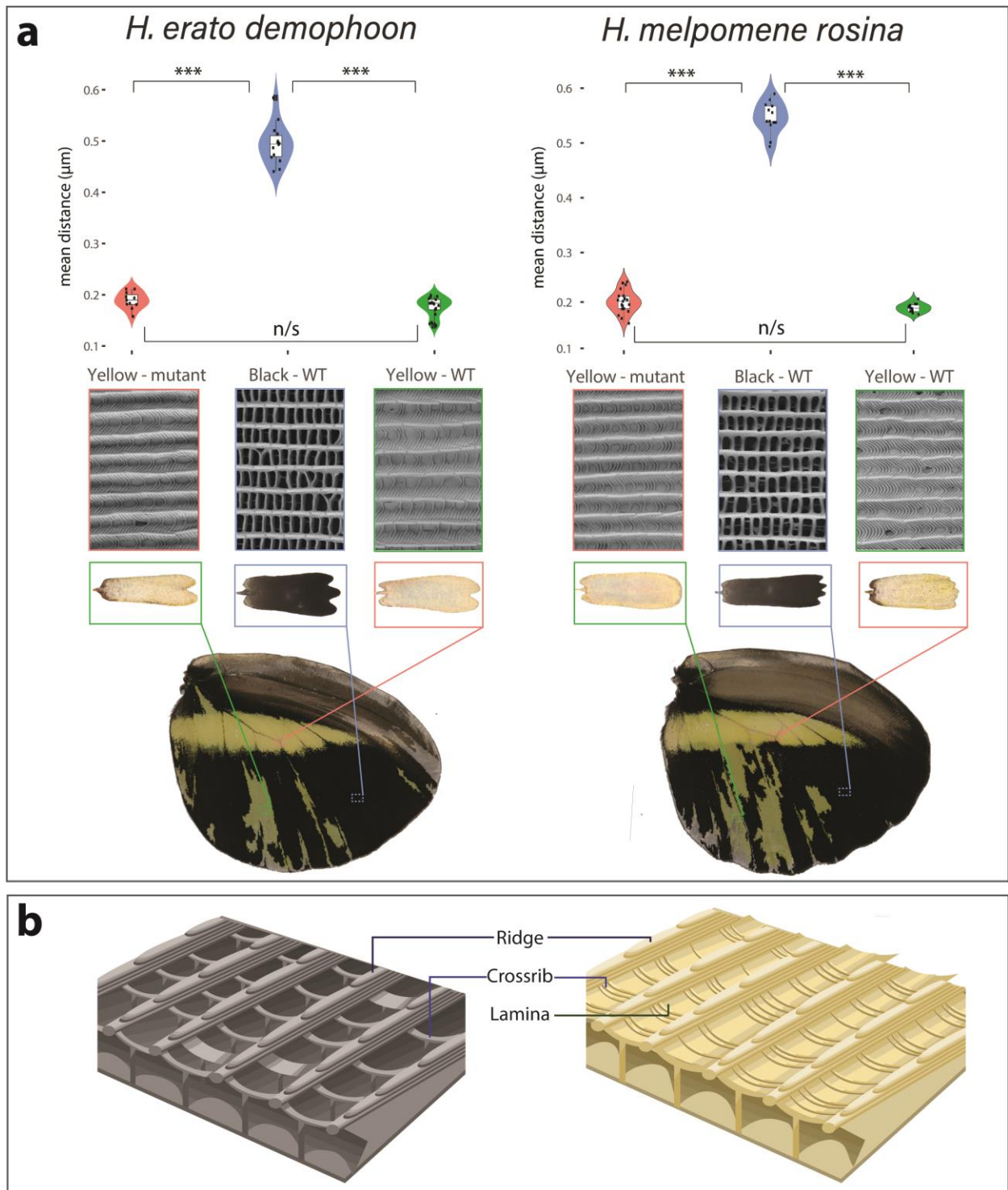
Figure 6 – Cortex protein localises throughout pupal hindwings in *H. erato demophoon*

(a) Cortex immunostaining reveals presence of Cortex across the hindwing of *H. erato demophoon*. DAPI (left) Cortex (middle) and merged channels (right) are shown. (b) Cortex localises as puncta in the developing pupal cells. Multiple puncta per cell are visible in the large polyploid nuclei (blue arrows) while single puncta localise to the uninuclear epithelium below (red arrows). Scale bar = 30µm.

282 ***Cortex* KO causes homeotic shifts in scale structure.**

283 Previous studies have shown an association between scale ultrastructure and pigmentation in *Heliconius*
284 butterflies (Concha et al., 2019; Gilbert et al., 1987; Zhang et al., 2017). With this in mind, we tested
285 whether ectopic yellow/white scales were accompanied by structural homeosis using Scanning Electron
286 Microscopy. To account for known positional effects on scale structure we compared wild-type and
287 mutant scales from homologous locations across the wing surface.

288 Ultrastructural differences are consistent with homeosis in *cortex* mutant scales in both *H. melpomene*
289 and *H. erato* (Figure 7). Cross-rib distance is the same between yellow wild-type and *cortex* mutant
290 scales, and significantly different between distally located wild-type black scales. A similar relationship
291 was observed for scale length in both species, but inter-ridge distance and scale width was consistent
292 with homeosis only in *H. melpomene* (Supplementary File 11 – Figure S11). A consistent difference
293 between all Type I scales (mutant and wild-type) is the presence of a lamina covering the inter-ridge
294 space (Figure 7b), suggesting this structure is an important morphological feature of yellow/white scales
295 (Matsuoka and Monteiro, 2018), and that *cortex* is necessary for the differentiation of lamellar tissue in
296 *Heliconius* scales.



297

Figure 7 – SEM reveals structural homeosis is induced in *cortex* KO scales.

Structural homeosis is induced in *cortex* KO scales in both *H. melpomene* and *H. erato*. Mutant and wild-type scale comparisons from homologous wing positions are shown, illustrating clear ultrastructural homeosis between wild-type and KO yellow scales. Mean cross-rib distance between wild-type and mutant yellow scales is not significantly different, while significantly different between both wild-type yellow and mutant yellow with wild-type black scales (Wilcoxon test, *** indicates $p < 0.001$).

298

299 **Discussion:**

300 ***Cortex* is a key scale cell specification gene**

301 The genetic locus containing the gene *cortex* represents a remarkable case of parallel evolution, where
302 repeated and independent mutations surrounding the gene are associated with shifts in scale
303 pigmentation state in at least 8 divergent species of Lepidoptera (Beldade et al., 2009; Nadeau et al.,
304 2016; Van Belleghem et al., 2017; VanKuren et al., 2019; van't Hof et al., 2019; Van't Hof et al., 2016).
305 While these studies have linked putative regulatory variation around *cortex* to the evolution of wing
306 patterns, its precise effect on scale cell identity and pigmentation has remained speculative until now.
307 Here, we demonstrate that *cortex* is a causative gene that specifies melanic and red (Type II and Type
308 III) scale cell identity in *Heliconius*, and acts by influencing both downstream pigmentation pathways
309 and scale cell ultrastructure. Moreover, our combination of expression studies and functional knock-
310 outs demonstrate that this gene acts as a key early scale cell specification switch across the wing surface
311 of *Heliconius* butterflies, and thus has the potential to generate much broader pattern variation than
312 previously described patterning genes.

313 While we have shown that *cortex* is a key scale cell specification gene, it remains unclear how a gene
314 with homology to the fizzy/cdc20 family of cell cycle regulators acts to modulate scale identity. In
315 *Drosophila*, Fizzy proteins are known to regulate APC/C activity through the degradation of cyclins,
316 leading to the arrest of mitosis (Raff et al., 2002). In particular, *fizzy-related* (*fzr*), induces a switch from
317 the mitotic cycle to the endocycle, allowing the development of polyploid follicle cells in *Drosophila*
318 ovaries (Schaeffer et al., 2004; Shcherbata, 2004). Similarly *cortex* has been shown to downregulate
319 cyclins during *Drosophila* female meiosis, through its interaction with the APC/C (Pesin and Orr-
320 Weaver, 2007; Swan and Schüpbach, 2007). Cortex Immunostainings show that Cortex protein
321 localises to the nucleus in *Heliconius* pupal wings, suggesting a possible interaction with the APC/C in
322 butterfly scale building cells. Ploidy levels in Lepidoptera scale cells have been shown to correlate with
323 pigmentation state, where increased ploidy and scale size lead to darker scales (Cho and Nijhout, 2013;
324 Iwata and Otaki, 2016). *cortex* may thus be modulating ploidy levels by inducing endoreplication cycles
325 in developing scale cells. However, we currently have no direct evidence for a causal relationship
326 between ploidy state and pigmentation output, and a mechanistic understanding of this relationship and
327 any role *cortex* may be playing in modulating ploidy levels will require future investigation.

328 ***Heliconius* wing patterning is controlled by interactions among major patterning genes**

329 Functional knockouts now exist for all the 4 major loci known to drive pigmentation differences in
330 *Heliconius* (Mazo-Vargas et al., 2017; Westerman et al., 2018; Zhang et al., 2017). These loci represent
331 the major switching points in the GRNs that are ultimately responsible for determining scales cell
332 identity. This work underscores the importance of two patterning loci, *cortex* and *WntA*, as master

333 regulators of scale cell identity. Both are upregulated early in wing development and have broad effects
334 on pattern variation (Concha et al., 2019; Nadeau et al., 2016). The signalling molecule *WntA* modulates
335 forewing band shape in *Heliconius* by delineating boundaries around patterns elements, and is expressed
336 in close association with future pattern elements (Concha et al., 2019; Martin et al., 2012). Unlike *cortex*
337 mutants, *WntA* KOs shift scale cell identity to all three cell Types (I, II and III), depending on genetic
338 background. Thus, *WntA* acts as a spatial patterning signal inducing or inhibiting colour in specific wing
339 elements, in contrast to *cortex*, which acts as an “on-off” switch across all scales on the butterfly wing.

340 Interestingly, *cortex* knockouts lead to shifts in scale fate irrespective of *WntA* expression. This suggests
341 either that *cortex* is required as an inductive signal to allow *WntA* to signal further melanisation, or that
342 two, independent ways to melanise a scale are available to the developing wing. The latter hypothesis
343 is supported by certain *H. erato* colour pattern *WntA* mutants, where even in putatively *cortex* positive
344 regions, scales are able to shift to Type I in the absence of *WntA* alone (Concha et al., 2019). This
345 suggests that while under certain conditions *cortex* is sufficient to induce the development of black
346 scales, *WntA* is also required as a further signal for melanisation in some genetic backgrounds. Under
347 this scenario, colour pattern morphs may be responding epistatically to different *WntA/cortex* alleles
348 present in their respective genetic backgrounds.

349 Under a simple model (Figure 8), *cortex* is one of the earliest regulators and sets scale differentiation to
350 a specific pathway switches between Type I (yellow/white) and Type II/III (black/red) scales. Thus, we
351 can envision a differentiating presumptive scale cell (PSC) receiving a Cortex input as becoming Type
352 II/III competent, with complete Type III differentiation occurring in the presence of *optix* expression
353 (Zhang et al., 2017). This is consistent with our data, which shows *cortex* is also required as a signal
354 for Type III (red) scales to properly develop. Several *cortex* mutant individuals had clones across red
355 pattern elements, and failed to properly develop red pigment. The development of red scales in
356 *Heliconius* butterflies is also dependent on expression of the transcription factor *optix* during mid-pupal
357 development (Lewis et al., 2019; Reed et al., 2011; Zhang et al., 2017). Therefore, *cortex* expression is
358 required for either downstream signalling to *optix*, or to induce a permissive scale morphology for the
359 synthesis and deposition of red pigment in future scales. *Cortex* is thus necessary for the induction of
360 Type III scale cells but insufficient for their proper development.

361 Conversely, a PSC lacking a Cortex input differentiates into a Type I scale, whose pigmentation state
362 depends on the presence of the transcription factor *aristaless1* (*all*), where *all* is responsible for
363 inducing a switch from yellow to white scales in *Heliconius* by affecting the deposition of the yellow
364 pigment 3-OHK (Westerman et al., 2018). The uptake of 3-OHK from the haemolymph occurs very
365 late in wing development, right before the adult ecloses (Reed et al., 2008). Our *cortex* crispants
366 revealed a shift to both yellow and white scales, with their appearance being positionally dependent;
367 more distally located scales generally switch to white, while more proximal scales become yellow

368 (Supplementary File 8 and 9). This pigmentation state is likely controlled by differences in *all*
369 expression varying between wing sections in different ways across races.

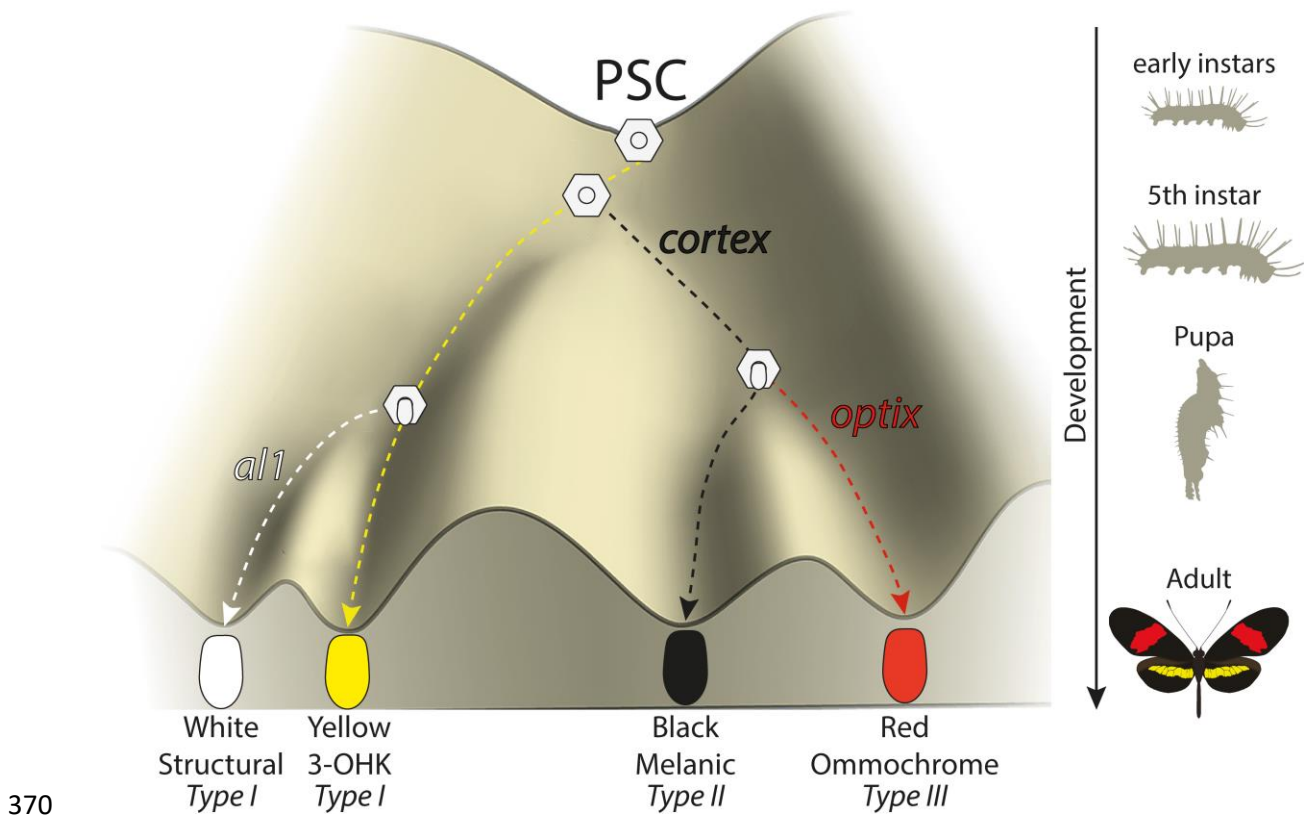


Figure 8 – Expression of key genes affect scale fate decisions and influence downstream pigmentation state

During early instar development, wing disc cells differentiate into presumptive scale cells (PSCs). Throughout 5th instar growth, PSCs express key scale cell specification genes such as *cortex*, which induce differentiation into Type II (*optix* -) scales or Type III (*optix* +) scales. In the absence of *cortex*, scale cells differentiate into Type I scales which differ in pigmentation state based on 3-OHK synthesis controlled by *aristalless1* expression. Model based on the epigenetic landscape (Waddington).

371 However, the switch induced by Cortex under this model is likely not a simple binary toggle, and is
372 perhaps dependent on a given protein threshold or heterochrony in expression rather than
373 presence/absence, as we find that Cortex protein also localises to the presumptive yellow bar in
374 developing pupal wings. Moreover, the *RNA-seq* data presented suggests other linked genes may also
375 be playing a role in controlling pattern switches between *Heliconius* races. In particular, we report the
376 presence of a bi-cistronic transcript containing the ORFs of the genes *dome* and *wash*, which are
377 differentially expressed during early pupal wing development. While a precise role for *dome/wash* in
378 wing patterning remains to be demonstrated, it raises the possibility that multiple linked genes co-
379 operate during *Heliconius* wing development to drive pattern diversity. It is noteworthy that in the
380 locally polymorphic *H. numata*, all wing pattern variation is controlled by inversions surrounding *cortex*

381 and *dome/wash*, both of which are also differentially expressed in *H. numata* (Saenko et al., 2019). This
382 raises the interesting possibility that evolution has favoured the interaction of multiple genes at the locus
383 that have since become locked into a supergene in *H. numata*.

384 **Conclusions:**

385 The utilization of ‘hotspots’ in evolution has become a recurring theme of evolutionary biology, with
386 several examples in which independent mutations surrounding the same gene have driven adaptive
387 evolution (e.g *Pitx1*, *Scute*) (Stern and Orgogozo, 2009). One proposed facilitator of such hotspots is
388 through the action of genes acting as “input-output” modules, whereby complex spatio-temporal
389 information is translated into a co-ordinated cell differentiation program, in a simple switch like manner.
390 One prediction of the nature of such genes would be a switch-like behaviour such as that observed for
391 *cortex* in this study, as well as the presence of a complex modular *cis*-regulatory architecture
392 surrounding the gene that is able to integrate the complex upstream positional information into the
393 switch-like output. A conserved feature of the *cortex* locus in Lepidoptera is the presence of large
394 intergenic regions surrounding the gene, with evidence these may be acting as modular *cis*-regulatory
395 switches in *Heliconius* (Enciso-Romero et al., 2017; Van Belleghem et al., 2017), fitting the predicted
396 structure of input-output genes. Unlike canonical input-output loci however, *cortex* expression appears
397 not to be restricted to any particular colour pattern element in any given species/race, and yet is capable
398 of producing a switch-like output (Type I vs Type II/III scales).

399 The genetic locus containing the gene *cortex* has now been implicated in driving wing patterning
400 differences in many divergent Lepidoptera, and represents one of the more striking cases of parallel
401 evolution to date. We have shown that it is spatially regulated during larval development, and yet shows
402 wing-wide cell fate phenotypes leading to a switch in scale cell fate. The amenability of *cortex* to
403 evolutionary change suggests it may be occupying an unusual position in the GRN underlying scale cell
404 identity, and may be acting as an input/output gene (Stern and Orgogozo, 2009) that integrates upstream
405 positional information into a simple on-off switch for scale differentiation. However, it is still unclear
406 how *cortex* mechanistically affects pigmentation differences, and given its widespread usage throughout
407 Lepidoptera, it is of general interest to understand its role in driving scale pigmentation.

408

409 **Materials and Methods**

410 **Butterfly husbandry**

411 *Heliconius* butterflies were collected in the tropical forests of Panama and Ecuador. Adults were
412 provided with an artificial diet of pollen/glucose solution supplemented with flowers of *Psiguria*,
413 *Lantana* and/or *Psychotria alata* according to availability. Females were provided with *Passiflora* plants
414 for egg laying (*P. menispermifolia* for *H. melpomene*, *P. biflora* for *H. erato* and *H. charithonia*, and
415 *P. vitifolia* for *H. hecale*). Eggs were collected daily, and caterpillars reared on fresh shoots of *P.*
416 *williamsi* (*melpomene*), *P. biflora* (*erato* and *charithonia*) and *P. vitifolia* for *H. hecale*. Late 5th (final)
417 instar, caterpillars were separated into individual pots in a temperature-monitored room for *RNA-seq*
418 experiments, where they were closely observed for the purpose of accurate developmental staging.

419 **Phylogenetic analysis of *domeless* and *cortex***

420 To identify orthologs of *dome* across the Lepidoptera we performed tBLASTn searches using the
421 previously annotated *H. melpomene* Hmel2 (Hm) and *H. erato demophoon* V1 (Hed) *dome* sequences
422 against the genomes of *Operophtera brumata* V1 (Ob), *Trichoplusia ni* Hi5.VO2 (Tn), *Bombyx mori*
423 ASM15162v1 (Bm), *Manduca sexta* 1.0 (Ms), *Plodia interpunctella* V1 (Pi), *Amyeolis transitella* V1
424 (At), *Phoebis sennae* V1.1 (Ps), *Bicyclus anynana* V1.2 (Ba), *Danaus plexippus* V3 (Dp), *Dryas iulia*
425 helico3 (Di), *Agraulis vanillae* helico3 (Av), *Heliconius erato lativitta* V1 (Hel) genomes found on
426 Lepbase (Challis et al., 2016). As a trichopteran outgroup we used a recently published Pacbio assembly
427 of *Stenopsyche tienmushanensis* (St) (Luo et al., 2018). Recovered amino acid translations were aligned
428 using clustal omega (F. et al., 2019). The resulting alignments were used to produce a phylogenetic tree
429 using PhyML (Guindon et al., 2010), based on a best fit model using AIC criterion (selected model was
430 JTT + G + I + F). The tree was visualised and re-rooted to the Trichopteran outgroup using FigTree.

431 To confirm *cortex* as a *cdc20* gene, we retrieved full-length protein homologs from TBLASTN searches
432 and used them to generate a curated alignment with MAFFT/Guidance2 with a column threshold of 0.5.
433 We then constructed a maximum-likelihood tree using W-IQ-TREE with the “Auto” function to find a
434 best-fit model of substitution.

435 **Tissue sampling and *RNA-Seq***

436 *H. melpomene rosina* and *H. erato demophoon* butterflies were collected around Gamboa, Panama; *H.*
437 *melpomene melpomene* and *H. erato hydara* butterflies were collected around Puerto Lara, Darien,
438 Panama. Methodology for sample preparation and sequencing was performed as previously described
439 (Hanly et al., 2019). The datasets generated and/or analysed during the current study are available in
440 the SRA repository (PRJNA552081). Reads from each species were aligned to the respective genome
441 assemblies Hmel2 (Davey et al., 2016) and Herato_demophoon_v1 (Van Belleghem et al., 2017),

442 available on using Hisat2 with default parameters (Kim et al., 2019). The genomes and annotations used
443 are publicly available at www.lepbase.org. Reads were counted with HTSeq-count in union mode
444 (Anders et al., 2015) and statistical analysis performed with the R package DESeq2 (Love et al., 2014),
445 using the GLMI;

446 ~ individual + compartment*race

447 (Compartments: Anterior Hindwing (HA), Posterior Hindwing (HPo)). *H. melpomene* and *H. erato*
448 were analysed separately; homology between genes was determined by reciprocal BLAST. Contrasts
449 were then extracted for comparison of race, compartment, and race given the effect of compartment,
450 alternating the race used as the base level.

451 ***In situ* hybridizations**

452 Fifth instar larval wing disks and whole mount *in situ* hybridizations were performed following a
453 published procedure (Martin and Reed, 2014) and imaged using a Leica S4E microscope (Leica
454 Microsystems). Riboprobe synthesis was performed using the following primers from a 5th instar wing
455 disc cDNA library extracted from *H. melpomene*:

456 Forward primer 5' – CCCGAGATTCTTTCAGCGAAAC -3' and Reverse primer 5' –
457 ACCGCTCCAACACCAAGAAG – 3'. Templates for riboprobes were designed by attaching a T7
458 promoter through PCR and performing a DIG labelled transcription reaction (Roche). The same *H.*
459 *melpomene* probe was used in all *in situ* hybridisation experiments. The resulting probe spanned from
460 Exon 2 to Exon 7 and was 841bp long.

461 **Immunohistochemistry and image analysis**

462 Pupal wings were dissected around 60 to 70 h post pupation in PBS and fixed at room temperature with
463 fix buffer (400 µl 4% paraformaldehyde, 600 µl PBS 2mM EGTA) for 30 min. Subsequent washes
464 were done in wash buffer (0.1% Triton-X 100 in PBS) before blocking the wings at 4°C in block buffer
465 (0.05 g Bovine Serum Albumin, 10 ml PBS 0.1% Triton-X 100). Wings were then incubated in primary
466 antibodies against Cortex (1:200, monoclonal rabbit anti-Cortex) at 4°C overnight, washed and added
467 in secondary antibody (1:500, donkey anti-rabbit IgG, AlexaFlour 555, ThermoFisher Scientific A-
468 31572). Before mounting, wings were incubated in DAPI with 50% glycerol overnight and finally
469 transferred to mounting medium (60% glycerol/ 40% PBS 2mM EGTA) for imaging.

470 Z-stacked 2-channelled confocal images were acquired using a Zeiss Cell Observer Spinning Disk
471 Confocal microscope. Image processing was done using FIJI plugins Trainable Weka Segmentation
472 and BioVoxxel (Arganda-Carreras et al., 2017; Brocher, Jan, 2014; Schindelin et al., 2012). Manual
473 tracing of nuclei was input for machine learning and processing of images to obtain final thresholded
474 images, then an overlay of Cortex puncta with DAPI nuclei staining identified regions of nuclei

475 containing Cortex puncta. Spatial analysis of image data was conducted using R software 4.0.0 package
476 Spatstat (Baddeley and Turner, 2005).

477 **CRISPR/Cas9 genome editing**

478 Guide RNAs were designed corresponding to GGN₂₀NGG sites located within the *cortex* coding region
479 using the program Geneious (Kearse et al., 2012). To increase target specificity, guides were checked
480 against an alignment of both *melpomene* and *erato* re-sequence data at the scaffolds containing the
481 *cortex* gene (Moest et al., 2020; Van Belleghem et al., 2017), and selected based on sequence
482 conservation across populations. Based on these criteria, each individual guide was checked against the
483 corresponding genome for off-target effects, using the default Geneious algorithm. Guide RNAs with
484 high conservation and low off-target scores were then synthesised following the protocol by Bassett
485 and Liu, 2014. Injections were performed following procedures described in Mazo-Vargas et al., 2017,
486 within 1-4 hours of egg laying. Several combinations of guide RNAs for separate exons at different
487 concentrations were used for different injection experiments (Supplementary File 7). For *H. charithonia*
488 we used the *H. erato* specific guides and for *H. hecale* we used the *H. melpomene* guides.

489 **Genotyping**

490 DNA was extracted from mutant leg tissue and amplified using oligonucleotides flanking the sgRNAs
491 target region (Supplementary File 6). PCR amplicons were column purified, subcloned into the pGEM-
492 T Easy Vector System (Promega) and sequenced on an ABI 3730 sequencer.

493 **Scanning Electron Microscopy (SEM) Imaging**

494 Individual scales from wild type and mutant regions of interest were collected by brushing the surface
495 of the wing with an eyelash tool, then dusted onto an SEM stub with double-sided carbon tape. Stubs
496 were then colour imaged under the Keyence VHX-5000 microscope for registration of scale type.
497 Samples were sputter-coated with one 12.5 nm layer of gold for improving sample conductivity. SEM
498 images were acquired on a FEI Teneo LV SEM, using secondary electrons (SE) and an Everhart-
499 Thornley detector (ETD) using a beam energy of 2.00 kV, beam current of 25 pA, and a 10 μ s dwell
500 time. Individual images were stitched using the Maps 3.10 software (ThermoFisher Scientific).

501 **Morphometrics analysis**

502 Morphometric measurements of scale widths and ridge distances were carried out on between 10 and
503 20 scales of each type, using a custom semi-automated R pipeline that derives ultrastructural
504 parameters from large SEM images (Day et al., 2019). Briefly, ridge spacing was assessed by Fourier
505 transforming intensity traces of the ridges acquired from the FIJI software (Schindelin et al.,
506 2012). Scale width was directly measured in FIJI by manually tracing a line, orthogonal to the ridges,
507 at the section of maximal width.

508 **Author Contributions**

509 C.D.J., L.L., J.J.H., A.M., and W.O.M. designed the research; L.L., J.J.H., L.S.L., A.R., I.A.W.,
510 C.C., C.W., J.M.W., J.F., H.A.C., L.R.B. performed research. L.L wrote the paper.

511 **Acknowledgements**

512 We thank Oscar Paneso, Elizabeth Evans, Rachel Crisp and Cruz Batista, for technical support with
513 rearing of butterflies and CRISPR larvae, and to Markus Möest, Steven Van Belleghem and Tim
514 Thurman for assistance with butterfly collection. We are also grateful to Krzysztof “Chris” Kozak and
515 Chi Yun for thoughtful discussions and feedback on the manuscript. We thank the GW Nanofabrication
516 and Imaging Center for enabling SEM, and in particular Christine Brantner and Anastas Popratiloff for
517 their technical assistance

518 **Competing interests**

519 The authors declare no competing interests.

520

521 **References**

- 522 Anders S, Pyl PT, Huber W. 2015. HTSeq—a Python framework to work with high-throughput
523 sequencing data. *Bioinformatics* **31**:166–169. doi:10.1093/bioinformatics/btu638
- 524 Arganda-Carreras I, Kaynig V, Rueden C, Eliceiri KW, Schindelin J, Cardona A, Sebastian Seung H.
525 2017. Trainable Weka Segmentation: a machine learning tool for microscopy pixel
526 classification. *Bioinformatics* **33**:2424–2426. doi:10.1093/bioinformatics/btx180
- 527 Aymone ACB, Valente VLS, de Araújo AM. 2013. Ultrastructure and morphogenesis of the wing
528 scales in *Heliconius erato phyllis* (Lepidoptera: Nymphalidae): What silvery/brownish
529 surfaces can tell us about the development of color patterning? *Arthropod Structure &*
530 *Development* **42**:349–359. doi:10.1016/j.asd.2013.06.001
- 531 Baddeley A, Turner R. 2005. spatstat: An R Package for Analyzing Spatial Point Patterns. *Journal of*
532 *Statistical Software* **12**:1–42. doi:10.18637/jss.v012.i06
- 533 Bassett A, Liu J-L. 2014. CRISPR/Cas9 mediated genome engineering in *Drosophila*. *Methods* **69**:128–
534 136. doi:10.1016/j.ymeth.2014.02.019
- 535 Beldade P, Saenko SV, Pul N, Long AD. 2009. A Gene-Based Linkage Map for *Bicyclus anynana*
536 Butterflies Allows for a Comprehensive Analysis of Synteny with the Lepidopteran Reference
537 Genome. *PLOS Genetics* **5**:e1000366. doi:10.1371/journal.pgen.1000366

- 538 Brocher, Jan. 2014. Qualitative and Quantitative Evaluation of Two New Histogram Limiting
539 Binarization Algorithms. *Computer Science Journals* **8**:30–48.
- 540 Brown KS. 1981. The Biology of Heliconius and Related Genera. *Annual Review of Entomology*
541 **26**:427–457. doi:10.1146/annurev.en.26.010181.002235
- 542 Challi RJ, Kumar S, Dasmahapatra KK, Jiggins CD, Blaxter M. 2016. Lepbase: the Lepidopteran
543 genome database. *bioRxiv* 056994. doi:10.1101/056994
- 544 Cho EH, Nijhout HF. 2013. Development of polyploidy of scale-building cells in the wings of *Manduca*
545 *sexta*. *Arthropod Struct Dev* **42**:37–46. doi:10.1016/j.asd.2012.09.003
- 546 Chu T, Henrion G, Haegeli V, Strickland S. 2001. Cortex, a *Drosophila* gene required to complete
547 oocyte meiosis, is a member of the Cdc20/fizzy protein family. *Genesis* **29**:141–152.
548 doi:10.1002/gene.1017
- 549 Concha C, Wallbank RWR, Hanly JJ, Fenner J, Livraghi L, Rivera ES, Paulo DF, Arias C, Vargas M,
550 Sanjeev M, Morrison C, Tian D, Aguirre P, Ferrara S, Foley J, Pardo-Diaz C, Salazar C, Linares
551 M, Massardo D, Counterman BA, Scott MJ, Jiggins CD, Papa R, Martin A, McMillan WO. 2019.
552 Interplay between Developmental Flexibility and Determinism in the Evolution of Mimetic
553 Heliconius Wing Patterns. *Current Biology* S0960982219313168.
554 doi:10.1016/j.cub.2019.10.010
- 555 Courtier-Orgogozo V, Arnoult L, Prigent SR, Wiltgen S, Martin A. 2020. Gephebase, a database of
556 genotype–phenotype relationships for natural and domesticated variation in Eukaryotes.
557 *Nucleic Acids Res* **48**:D696–D703. doi:10.1093/nar/gkz796
- 558 Davey JW, Chouteau M, Barker SL, Maroja L, Baxter SW, Simpson F, Merrill RM, Joron M, Mallet J,
559 Dasmahapatra KK, Jiggins CD. 2016. Major Improvements to the *Heliconius melpomene*
560 Genome Assembly Used to Confirm 10 Chromosome Fusion Events in 6 Million Years of
561 Butterfly Evolution. *G3: Genes, Genomes, Genetics* **6**:695–708. doi:10.1534/g3.115.023655
- 562 Day CR, Hanly JJ, Ren A, Martin A. 2019. Sub-micrometer insights into the cytoskeletal dynamics and
563 ultrastructural diversity of butterfly wing scales. *Dev Dyn* **248**:657–670. doi:10.1002/dvdy.63
- 564 Enciso-Romero J, Pardo-Díaz C, Martin SH, Arias CF, Linares M, McMillan WO, Jiggins CD, Salazar C.
565 2017. Evolution of novel mimicry rings facilitated by adaptive introgression in tropical
566 butterflies. *Molecular Ecology* **26**:5160–5172. doi:10.1111/mec.14277
- 567 F M, Ym P, J L, N B, T G, N M, P B, Arn T, Sc P, Rd F, R L. 2019. The EMBL-EBI search and sequence
568 analysis tools APIs in 2019. *Nucleic Acids Res* **47**:W636–W641. doi:10.1093/nar/gkz268
- 569 Finkbeiner SD, Fishman DA, Osorio D, Briscoe AD. 2017. Ultraviolet and yellow reflectance but not
570 fluorescence is important for visual discrimination of conspecifics by *Heliconius erato*.
571 *Journal of Experimental Biology* **220**:1267–1276. doi:10.1242/jeb.153593

- 572 Gilbert LE, Forrest HS, Schultz TD, Harvey DJ. 1987. Correlations of ultrastructure and pigmentation
573 suggest how genes control development of wing scales of Heliconius butterflies. *The Journal*
574 *of research on the Lepidoptera (USA)*.
- 575 Greenstein ME. 1972. The ultrastructure of developing wings in the giant silkmoth, *Hyalophora*
576 *cecropia*. II. Scale-forming and socket-forming cells. *J Morphol* **136**:23–51.
577 doi:10.1002/jmor.1051360103
- 578 Guindon S, Dufayard J-F, Lefort V, Anisimova M, Hordijk W, Gascuel O. 2010. New Algorithms and
579 Methods to Estimate Maximum-Likelihood Phylogenies: Assessing the Performance of
580 PhyML 3.0. *Systematic Biology* **59**:307–321. doi:10.1093/sysbio/syq010
- 581 Hanly JJ, Wallbank RWR, McMillan WO, Jiggins CD. 2019. Conservation and flexibility in the gene
582 regulatory landscape of heliconiine butterfly wings. *EvoDevo* **10**:15. doi:10.1186/s13227-
583 019-0127-4
- 584 Henke K, Pohley H-J. 1952. Differentielle Zellteilungen und Polyploidie bei der Schuppenbildung der
585 Mehlmotte *Ephestia kühniella* Z. *Zeitschrift für Naturforschung B* **7**:65–79. doi:10.1515/zn-
586 1952-0201
- 587 Huber B, Whibley A, Poul YL, Navarro N, Martin A, Baxter S, Shah A, Gilles B, Wirth T, McMillan WO,
588 Joron M. 2015. Conservatism and novelty in the genetic architecture of adaptation in
589 *Heliconius* butterflies. *Heredity* **114**:515–524. doi:10.1038/hdy.2015.22
- 590 Ito K, Katsuma S, Kuwazaki S, Jouraku A, Fujimoto T, Sahara K, Yasukochi Y, Yamamoto K, Tabunoki H,
591 Yokoyama T, Kadono-Okuda K, Shimada T. 2016. Mapping and recombination analysis of two
592 moth colour mutations, Black moth and Wild wing spot, in the silkworm *Bombyx mori*.
593 *Heredity* **116**:52–59. doi:10.1038/hdy.2015.69
- 594 Iwata M, Otaki JM. 2016. Spatial patterns of correlated scale size and scale color in relation to color
595 pattern elements in butterfly wings. *Journal of Insect Physiology* **85**:32–45.
596 doi:10.1016/j.jinsphys.2015.11.013
- 597 Jiggins CD. 2017. *The Ecology and Evolution of Heliconius Butterflies*. Oxford University Press.
- 598 Jiggins CD, McMillan WO. 1997. The genetic basis of an adaptive radiation: warning colour in two
599 *Heliconius* species. *Proc Biol Sci* **264**:1167–1175. doi:10.1098/rspb.1997.0161
- 600 Joron M, Papa R, Beltrán M, Chamberlain N, Mavárez J, Baxter S, Abanto M, Bermingham E,
601 Humphray SJ, Rogers J, Beasley H, Barlow K, H. ffrench-Constant R, Mallet J, McMillan WO,
602 Jiggins CD. 2006. A Conserved Supergene Locus Controls Colour Pattern Diversity in
603 *Heliconius* Butterflies. *PLoS Biol* **4**:e303. doi:10.1371/journal.pbio.0040303
- 604 Kearse M, Moir R, Wilson A, Stones-Havas S, Cheung M, Sturrock S, Buxton S, Cooper A, Markowitz S,
605 Duran C, Thierer T, Ashton B, Meintjes P, Drummond A. 2012. Geneious Basic: an integrated

- 606 and extendable desktop software platform for the organization and analysis of sequence
607 data. *Bioinformatics* **28**:1647–1649. doi:10.1093/bioinformatics/bts199
- 608 Kim D, Paggi JM, Park C, Bennett C, Salzberg SL. 2019. Graph-based genome alignment and
609 genotyping with HISAT2 and HISAT-genotype. *Nat Biotechnol* **37**:907–915.
610 doi:10.1038/s41587-019-0201-4
- 611 Koch PB. 1993. Production of [14C]-Labeled 3-Hydroxy-L-Kynurenine in a Butterfly, *Heliconius*
612 *charitonia* L. (Heliconidae), and Precursor Studies in Butterfly Wing Ommatins. *Pigment Cell*
613 *Research* **6**:85–90. doi:10.1111/j.1600-0749.1993.tb00586.x
- 614 Kronforst MR, Papa R. 2015. The Functional Basis of Wing Patterning in *Heliconius* Butterflies: The
615 Molecules Behind Mimicry. *Genetics* **200**:1–19. doi:10.1534/genetics.114.172387
- 616 Lamas G, editor. 2004. Atlas Of Neotropical Lepidoptera: Checklist Pt. 4a Hesperioidea-papilionoidea.
617 Gainesville: Scientific Pub.
- 618 Lewis JJ, Geltman RC, Pollak PC, Rondem KE, Belleghem SMV, Hubisz MJ, Munn PR, Zhang L, Benson
619 C, Mazo-Vargas A, Danko CG, Counterman BA, Papa R, Reed RD. 2019. Parallel evolution of
620 ancient, pleiotropic enhancers underlies butterfly wing pattern mimicry. *PNAS* **116**:24174–
621 24183. doi:10.1073/pnas.1907068116
- 622 Lopes da Silva C. 2015. Genetics of diversification: a hotspot locus for pigmentation evolution
623 (Masters Thesis). Lisboa: Universidad de Lisboa.
- 624 Love MI, Huber W, Anders S. 2014. Moderated estimation of fold change and dispersion for RNA-seq
625 data with DESeq2. *Genome Biol* **15**:550. doi:10.1186/s13059-014-0550-8
- 626 Luo S, Tang M, Frandsen PB, Stewart RJ, Zhou X. 2018. The genome of an underwater architect, the
627 caddisfly *Stenopsyche tienmushanensis* Hwang (Insecta: Trichoptera). *Gigascience* **7**.
628 doi:10.1093/gigascience/giy143
- 629 Martin A, Courtier-Orgogozo V. 2017. Morphological Evolution Repeatedly Caused by Mutations in
630 Signaling Ligand Genes In: Sekimura T, Nijhout HF, editors. Diversity and Evolution of
631 Butterfly Wing Patterns: An Integrative Approach. Singapore: Springer. pp. 59–87.
632 doi:10.1007/978-981-10-4956-9_4
- 633 Martin A, Papa R, Nadeau NJ, Hill RI, Counterman BA, Halder G, Jiggins CD, Kronforst MR, Long AD,
634 McMillan WO, Reed RD. 2012. Diversification of complex butterfly wing patterns by
635 repeated regulatory evolution of a Wnt ligand. *Proc Natl Acad Sci USA* **109**:12632–12637.
636 doi:10.1073/pnas.1204800109
- 637 Martin A, Reed RD. 2014. Wnt signaling underlies evolution and development of the butterfly wing
638 pattern symmetry systems. *Developmental Biology* **395**:367–378.
639 doi:10.1016/j.ydbio.2014.08.031

- 640 Matsuoka Y, Monteiro A. 2018. Melanin Pathway Genes Regulate Color and Morphology of Butterfly
641 Wing Scales. *Cell Reports* **24**:56–65. doi:10.1016/j.celrep.2018.05.092
- 642 Mazo-Vargas A, Concha C, Livraghi L, Massardo D, Wallbank RWR, Zhang L, Papador JD, Martinez-
643 Najera D, Jiggins CD, Kronforst MR, Breuker CJ, Reed RD, Patel NH, McMillan WO, Martin A.
644 2017. Macroevolutionary shifts of WntA function potentiate butterfly wing-pattern diversity.
645 *PNAS* **114**:10701–10706. doi:10.1073/pnas.1708149114
- 646 Moest M, Belleghem SMV, James JE, Salazar C, Martin SH, Barker SL, Moreira GRP, Mérot C, Joron M,
647 Nadeau NJ, Steiner FM, Jiggins CD. 2020. Selective sweeps on novel and introgressed
648 variation shape mimicry loci in a butterfly adaptive radiation. *PLOS Biology* **18**:e3000597.
649 doi:10.1371/journal.pbio.3000597
- 650 Nadeau NJ. 2016. Genes controlling mimetic colour pattern variation in butterflies. *Current Opinion*
651 *in Insect Science, Global change biology * Molecular physiology* **17**:24–31.
652 doi:10.1016/j.cois.2016.05.013
- 653 Nadeau NJ, Pardo-Diaz C, Whibley A, Supple MA, Saenko SV, Wallbank RWR, Wu GC, Maroja L,
654 Ferguson L, Hanly JJ, Hines H, Salazar C, Merrill RM, Dowling AJ, ffrench-Constant RH,
655 Llaurens V, Joron M, McMillan WO, Jiggins CD. 2016. The gene cortex controls mimicry and
656 crypsis in butterflies and moths. *Nature* **534**:106–110. doi:10.1038/nature17961
- 657 Pesin JA, Orr-Weaver TL. 2007. Developmental Role and Regulation of cortex, a Meiosis-Specific
658 Anaphase-Promoting Complex/Cyclosome Activator. *PLOS Genetics* **3**:e202.
659 doi:10.1371/journal.pgen.0030202
- 660 Prud'homme B, Gompel N, Carroll SB. 2007. Emerging principles of regulatory evolution. *PNAS*
661 **104**:8605–8612. doi:10.1073/pnas.0700488104
- 662 Raff JW, Jeffers K, Huang J. 2002. The roles of Fzy/Cdc20 and Fzr/Cdh1 in regulating the destruction
663 of cyclin B in space and time. *J Cell Biol* **157**:1139–1149. doi:10.1083/jcb.200203035
- 664 Reed RD, McMillan WO, Nagy LM. 2008. Gene expression underlying adaptive variation in *Heliconius*
665 wing patterns: non-modular regulation of overlapping cinnabar and vermilion prepatterns.
666 *Proc Biol Sci* **275**:37–46. doi:10.1098/rspb.2007.1115
- 667 Reed RD, Papa R, Martin A, Hines HM, Counterman BA, Pardo-Diaz C, Jiggins CD, Chamberlain NL,
668 Kronforst MR, Chen R, Halder G, Nijhout HF, McMillan WO. 2011. optix drives the repeated
669 convergent evolution of butterfly wing pattern mimicry. *Science* **333**:1137–1141.
670 doi:10.1126/science.1208227
- 671 Rosser N, Phillimore AB, Huertas B, Willmott KR, Mallet J. 2012. Testing historical explanations for
672 gradients in species richness in heliconiine butterflies of tropical America: DIVERSIFICATION

- 673 OF BUTTERFLIES. *Biological Journal of the Linnean Society* **105**:479–497. doi:10.1111/j.1095-
674 8312.2011.01814.x
- 675 Saenko SV, Chouteau M, Piron-Prunier F, Blugeon C, Joron M, Llaurens V. 2019. Unravelling the
676 genes forming the wing pattern supergene in the polymorphic butterfly *Heliconius numata*.
677 *Evodevo* **10**:16. doi:10.1186/s13227-019-0129-2
- 678 Schaeffer V, Althausen C, Shcherbata HR, Deng W-M, Ruohola-Baker H. 2004. Notch-Dependent
679 Fizzy-Related/Hec1/Cdh1 Expression Is Required for the Mitotic-to-Endocycle Transition in
680 *Drosophila* Follicle Cells. *Current Biology* **14**:630–636. doi:10.1016/j.cub.2004.03.040
- 681 Schindelin J, Arganda-Carreras I, Frise E, Kaynig V, Longair M, Pietzsch T, Preibisch S, Rueden C,
682 Saalfeld S, Schmid B, Tinevez J-Y, White DJ, Hartenstein V, Eliceiri K, Tomancak P, Cardona A.
683 2012. Fiji: an open-source platform for biological-image analysis. *Nat Methods* **9**:676–682.
684 doi:10.1038/nmeth.2019
- 685 Shcherbata HR. 2004. The mitotic-to-endocycle switch in *Drosophila* follicle cells is executed by
686 Notch-dependent regulation of G1/S, G2/M and M/G1 cell-cycle transitions. *Development*
687 **131**:3169–3181. doi:10.1242/dev.01172
- 688 Stern DL, Orgogozo V. 2009. Is Genetic Evolution Predictable? *Science* **323**:746–751.
689 doi:10.1126/science.1158997
- 690 Swan A, Schüpbach T. 2007. The Cdc20 (Fzy)/Cdh1-related protein, Cort, cooperates with Fzy in
691 cyclin destruction and anaphase progression in meiosis I and II in *Drosophila*. *Development*
692 **134**:891–899. doi:10.1242/dev.02784
- 693 Thayer RC, Allen FI, Patel NH. 2020. Structural color in *Junonia* butterflies evolves by tuning scale
694 lamina thickness. *eLife* **9**:e52187. doi:10.7554/eLife.52187
- 695 Turner JRG. 1981. Adaptation and Evolution in *Heliconius*: A Defense of NeoDarwinism. *Annual*
696 *Review of Ecology and Systematics* **12**:99–121. doi:10.1146/annurev.es.12.110181.000531
- 697 Van Belleghem SM, Rastas P, Papanicolaou A, Martin SH, Arias CF, Supple MA, Hanly JJ, Mallet J,
698 Lewis JJ, Hines HM, Ruiz M, Salazar C, Linares M, Moreira GRP, Jiggins CD, Counterman BA,
699 McMillan WO, Papa R. 2017. Complex modular architecture around a simple toolkit of wing
700 pattern genes. *Nature Ecology & Evolution* **1**:1–12. doi:10.1038/s41559-016-0052
- 701 VanKuren NW, Massardo D, Nallu S, Kronforst MR. 2019. Butterfly mimicry polymorphisms highlight
702 phylogenetic limits of gene re-use in the evolution of diverse adaptations. *Mol Biol Evol.*
703 doi:10.1093/molbev/msz194
- 704 Van't Hof AE, Campagne P, Rigden DJ, Yung CJ, Lingley J, Quail MA, Hall N, Darby AC, Saccheri IJ.
705 2016. The industrial melanism mutation in British peppered moths is a transposable
706 element. *Nature* **534**:102–105. doi:10.1038/nature17951

- 707 van't Hof AE, Reynolds LA, Yung CJ, Cook LM, Saccheri IJ. 2019. Genetic convergence of industrial
708 melanism in three geometrid moths. *Biology Letters* **15**:20190582.
709 doi:10.1098/rsbl.2019.0582
- 710 Westerman EL, VanKuren NW, Massardo D, Tenger-Trolander A, Zhang W, Hill RI, Perry M, Bayala E,
711 Barr K, Chamberlain N, Douglas TE, Buerkle N, Palmer SE, Kronforst MR. 2018. Aristaless
712 Controls Butterfly Wing Color Variation Used in Mimicry and Mate Choice. *Curr Biol* **28**:3469-
713 3474.e4. doi:10.1016/j.cub.2018.08.051
- 714 Zhang L, Mazo-Vargas A, Reed RD. 2017. Single master regulatory gene coordinates the evolution
715 and development of butterfly color and iridescence. *PNAS* **114**:10707–10712.
716 doi:10.1073/pnas.1709058114